Journal of Statistical Models and Methods (2026)
2(1), 1–22, https://doi.org/10.65905/ny33vy73

AdvantaCore Scientific Publishing

Article Type: Research article

Several Properties and Estimation of a New Generalized Lomax Distribution with Applications to COVID-19 Data

Abdulkareem M. Basheer

Faculty of Administrative Sciences, Albaydha University, Albaydha, Yemen

Corresponding Author
Abdulkareem M. Basheer
abdulkareembasheer@baydaauniv.net

Article History

Received: 24 January 2026
Revised: 26 March 2026
Accepted: 03 April 2026

Keywords
Lomax distribution;
Modified alpha power transformation;
Moments;
Entropies;
Maximum likelihood estimation

Abstract

The main goal of this paper is to provide a new version of the Lomax distribution by introducing an additional shape parameter to enhance its adaptability. The modified alpha power transformed methodology is employed to develop the new version. Various structural properties of the new model are derived, comprising the quantile function, some moments, Lorenz and Bonferroni curves, entropies, order statistics, and stress-strength reliability. The parameters of the new version of the Lomax distribution are estimated utilizing the maximum likelihood estimation technique. A simulation analysis is performed to assess the effectiveness of the estimators obtained from the novel model, applying criteria such as mean squared error and bias. Three distinct applications related to COVID-19 and engineering data are employed to demonstrate the flexibility of the model.

1 Introduction

Lomax [1] proposed a two-parameter lifetime distribution, known as the Lomax (Lo) distribution (Pareto distribution of the second kind). The cumulative distribution function (CDF) and probability density function (PDF) of the Lo distribution are, respectively, given by

$$G(y) = 1 - (1 + \beta y)^{-\theta}, \qquad y > 0, \beta, \theta > 0 \tag{1}$$

and

$$g(y) = \beta\theta(1 + \beta y)^{-\theta-1}, \qquad y > 0, \beta, \theta > 0, \tag{2}$$

where β is the scale parameter and θ is the shape parameter. Lomax [1] used the distribution to analyze business failure data. Many authors studied the properties and estimation of the Lo distribution, as mentioned in Ghitany et al. [2].

Recently, several authors suggested numerous generalizations of the Lo distribution to increase its flexibility, such as the beta Lo by Rajab et al. [3], the transmuted Lo by Ashour and Eltehiwy [4], the exponential Lo by El Bassiouny et al. [5], the Gumbel Lo by Tahir et al. [6], the logistic Lo by Cordeiro et al. [7], the exponentiated Weibull Lo by Hassan and Abd-Allah [8], the generalization of Lo by Elgohari and Yousof [9], the topp Leone Kumaraswamy Lo by Ibrahim et al. [10], the transmuted generalized Lo by Abu El Azm et al. [11], the minimum Lindley Lo by Khan et al. [12], the Maxwell Lo by Abiodun et al. [13], a new Shifted Lo-X by Atchadé et al. [14], the weighted T-X power Lo by Abd Elgawad et al. [15], and the Pareto Lo by Afify et al. [16].

Copyright © 2026 by the author. Published under Creative Commons Attribution (CC BY) license.

Moreover, Mahdavi and Kundu [17] introduced a modification to the underlying CDF by incorporating an additional parameter to generate a range of distributions. This approach is referred to as the alpha power transformation (APT). If $G(y)$ represents the CDF of any distribution, then the CDF and PDF of the APT can be expressed as

$$F_{APT}(y) = \begin{cases} \frac{\alpha^{G(y)}-1}{\alpha-1}, & \alpha > 0, \alpha \neq 1 \\ G(y), & \alpha = 1 \end{cases} \tag{3}$$

and

$$f_{APT}(y) = \begin{cases} \frac{\log(\alpha)}{\alpha-1} g(y)\alpha^{G(y)}, & \alpha > 0, \alpha \neq 1 \\ g(y), & \alpha = 1. \end{cases} \tag{4}$$

Also, Alotaibi et al. [18] proposed a modification to the APT method and called it the modified APT (MAPT) method, with the following CDF and PDF

$$F_{MAPT}(y) = \begin{cases} \frac{\alpha^{G(y)}-1}{(\alpha-1)(1+\alpha-\alpha^{G(y)})}, & \alpha > 0, \alpha \neq 1 \\ G(y), & \alpha = 1 \end{cases} \tag{5}$$

and

$$f_{MAPT}(y) = \begin{cases} \frac{\log(\alpha)g(y)\alpha^{1+G(y)}}{(\alpha-1)(1+\alpha-\alpha^{G(y)})^2}, & \alpha > 0, \alpha \neq 1 \\ g(y), & \alpha = 1. \end{cases} \tag{6}$$

Many papers have recently studied the APT and MAPT, such as: APT Weibull by Nassar et al. [19, 20], APT Gompertz by Eghwerido et al. [21], APT inverse Lindley by Dey et al. [22], APT inverse Weibull by Basheer et al. [23, 24], Marshall–Olkin AP Weibull by Almetwally et al. [25], APT inverse Lo by ZeinEldin et al. [26], APT Lo by Maruthan et al. [27], APT exponentiated new Weibull-Pareto by Klakattawi et al. [28], new APT Pareto by Alsolmi et al. [29], APT generalized Pareto by Bleed et al. [30], MAPT Weibull by Alotaibi et al. [31], MAPT Kumaraswamy by Basheer et al. [32], and MAPT inverse Lindley by Basheer [33].

The following reasons motivate the proposed model: (1) Introducing the MAPT Lo (MAPTLo) as a novel three-parameter model based on the MAPT distribution family. (2) The newly suggested model is very flexible. (3) It is possible to compute several statistical features, comprising the moments, moment generating function, incomplete moments, conditional moment, mean residual life, stress-strength reliability, and so on. (4) The parameters of the MAPTLo distribution can be estimated via the maximum likelihood estimation (MLE) approach.

The remainder of the paper is structured as follows: In Section 2, we present the MAPTLo distribution. In Section 3, some useful statistical properties of the MAPTLo distribution are discussed. In Section 4, some reliability functions of the MAPTLo distribution are studied. The performance of the MLE method is discussed through a simulation study in Section 5. The MAPTLo distribution is implemented on three real datasets, and the outcomes are shown in Section 6. Finally, the paper is concluded in Section 7.

2 Modified Alpha Power Transformed Lomax Distribution

By incorporating the CDF of the Lo distribution expressed in (1) into the CDF of the MAPT distribution given in (5), we obtain the CDF of a new distribution denoted as the MAPTLo $(y; \alpha, \beta, \theta)$ distribution,

given by

$$F_{MAPTLo}(y) = \frac{\alpha^{1-(1+\beta y)^{-\theta}} - 1}{(\alpha - 1)(1 + \alpha - \alpha^{1-(1+\beta y)^{-\theta}})}, \tag{7}$$

and the related PDF is displayed by

$$f_{MAPTLo}(y) = \frac{\alpha\beta\theta \log(\alpha)(1 + \beta y)^{-(\theta+1)}\alpha^{1-(1+\beta y)^{-\theta}}}{(\alpha - 1)(1 + \alpha - \alpha^{1-(1+\beta y)^{-\theta}})^2}. \tag{8}$$

Many properties of the MAPTLo distribution depend on the PDF, so we expand Eq. (8) of the PDF by using the power series

$$\alpha^H = \sum_{s=0}^{\infty} \frac{(\log \alpha)^s H^s}{s!}, \tag{9}$$

and the expansion of generalized binomial

$$(1 - H)^{-2} = \sum_{j=0}^{\infty}(j + 1)H^j, |H| < 1 \quad and \quad (1 - H)^s = \sum_{k=0}^{s}(-1)^k \binom{s}{k} H^k, s \in N. \tag{10}$$

Applying Eqs. (9)–(10) to Eq. (8), we obtain the expansion of the PDF as

$$f_{MAPTLo}(y) = \sum_{s=0}^{\infty}\sum_{k=0}^{s} \Upsilon_{s,k} g(y; \beta, (1 + k)\theta), \tag{11}$$

where $g(y; \beta, (1 + k)\theta) = \beta(1 + k)\theta(1 + \beta y)^{-(1+k)\theta-1}$ is the PDF of the Lo distribution with parameters β and $(k + 1)\theta$, and

$$\Upsilon_{s,k} = \sum_{j=0}^{\infty} \frac{(-1)^k \alpha(\log \alpha)^{s+1}(j + 1)^{s+1}}{(\alpha^2 - 1)(\alpha + 1)^{j+1}(s - k)!(1 + k)!}.$$

Figure 1 include several types of PDF shapes. It shows that the Figure (a) is decreasing, Figure (b) is increasing, and Figure (c) is unimodal.

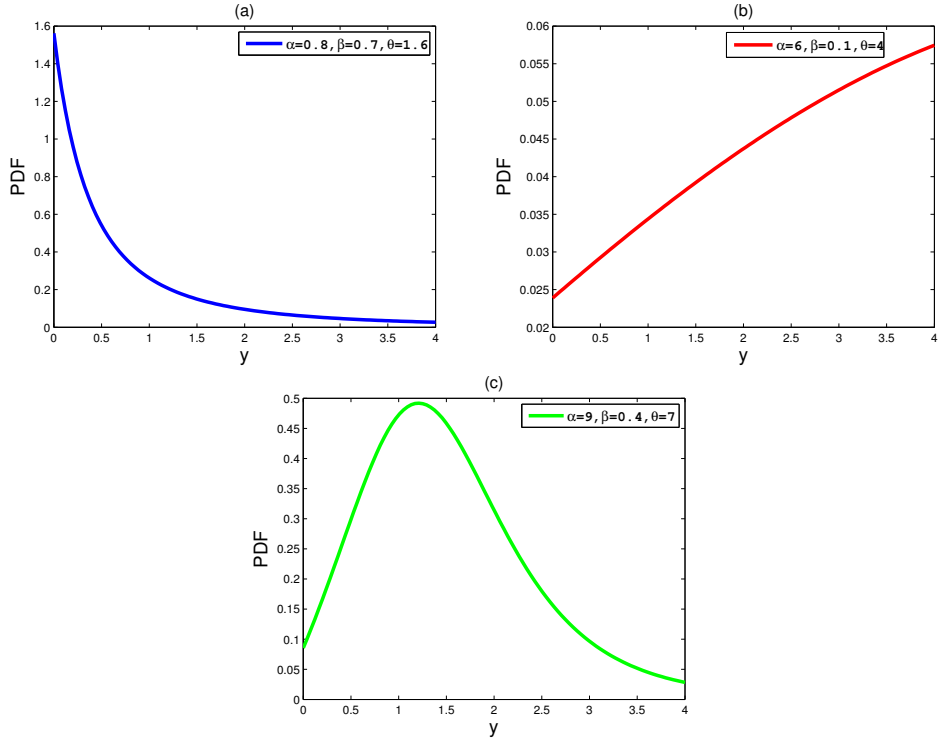


Figure 1: Some shapes of PDF.

Also, the behavior of PDF of MAPTLo distribution is investigated as

$$\lim_{y\to 0} f(y) = \frac{\beta\theta\log(\alpha)}{\alpha(\alpha-1)}, \alpha \neq 1 \qquad \text{and} \qquad \lim_{y\to\infty} f(y) = 0.$$

3 Statistical properties

Within this part, we will derive the quantile function, some moments, order statistics, and entropies of the MAPTLo distribution.

3.1 Quantile function

By using the Eq.(7), we can obtain the quantile function of the MAPTLo distribution as

$$y_q = Q_{MAPTLo}(q) = \frac{1}{\beta}\left\{\left[1 - \frac{\log\left(\frac{q(\alpha^2-1)+1}{q(\alpha-1)+1}\right)}{\log\alpha}\right]^{\frac{-1}{\theta}} - 1\right\}, \qquad 0 < q < 1. \tag{12}$$

From Eq. (12), we can obtain some quantiles such as $y_{0.25}$, $y_{0.50}$, and $y_{0.75}$. To generate samples from the MAPTLo distribution, we can use Eq. (12).

3.2 Moments

The r^{th} moment of the MAPTLo distribution can be formulated as

$$\begin{aligned}
\acute{\mu}_r = E(Y^r) &= \int_0^\infty y^r f(y;\alpha,\beta,\theta)dy \\
&= \sum_{s=0}^{\infty}\sum_{k=0}^{s} \Upsilon_{s,k} \int_0^\infty y^r g(y;\beta,(1+k)\theta)dy \\
&= \sum_{s=0}^{\infty}\sum_{k=0}^{s} \Upsilon_{s,k} \int_0^\infty y^r \beta\theta(1+k)(1+\beta y)^{-(1+k)\theta-1}dy \\
&= \sum_{s=0}^{\infty}\sum_{k=0}^{s} \Upsilon_{s,k} \frac{\Gamma(r+1)(1+k)\theta\Gamma((1+k)\theta-r)}{\beta^r\Gamma((1+k)\theta+1)} \\
&= \sum_{s=0}^{\infty}\sum_{k=0}^{s} \Upsilon_{s,k} \frac{r!\Gamma((1+k)\theta-r)}{\beta^r\Gamma((1+k)\theta)}, \qquad (1+k)\theta > r.
\end{aligned} \tag{13}$$

From Eq. (13), we can obtain some moments such as the mean, variance, skewness, and kurtosis. Also, the behaviors of some moments can be effortlessly viewed through Figures 2 and 3. The inverse moment (IM) of the MAPTLo distribution is obtained by replacing (r) with $(-r)$ in Eq. (13).

The moment generating function of the MAPTLo distribution can be formulated as

$$M_Y(t) = \int_0^\infty e^{ty} f(y)dy = \sum_{r=0}^{\infty}\frac{t^r}{r!}\int_0^\infty y^r f(y)dy = \sum_{r=0}^{\infty}\frac{t^r}{r!}E(Y^r). \tag{14}$$

The characteristic function of the MAPTLo distribution is obtained by replacing (t) with (it) in Eq. (14) as

$$M_Y(it) = \sum_{r=0}^{\infty}\frac{(it)^r E(Y^r)}{r!}. \tag{15}$$

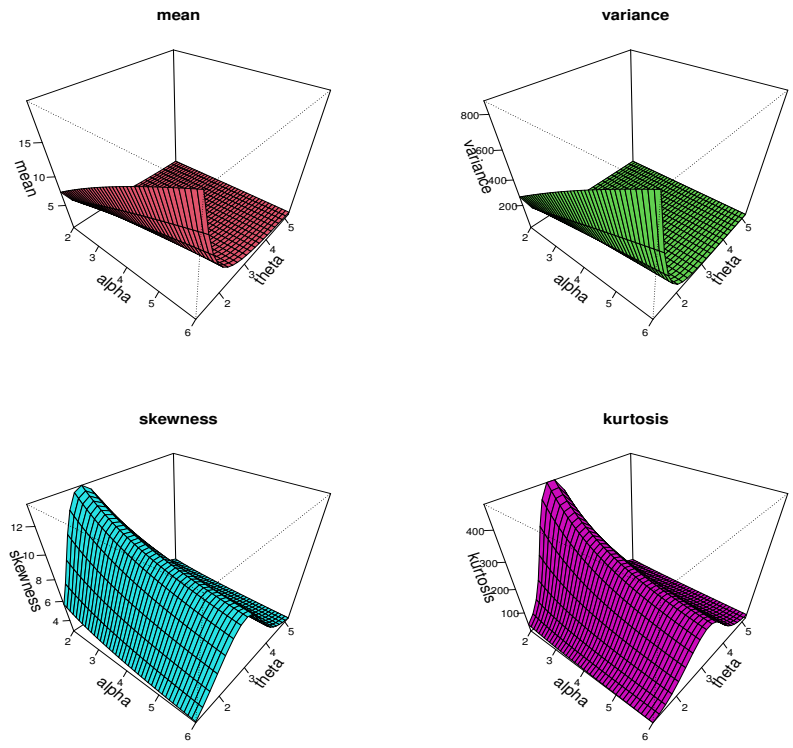


Figure 2: Moments for the MAPTLo distribution at $\beta = 0.8$.

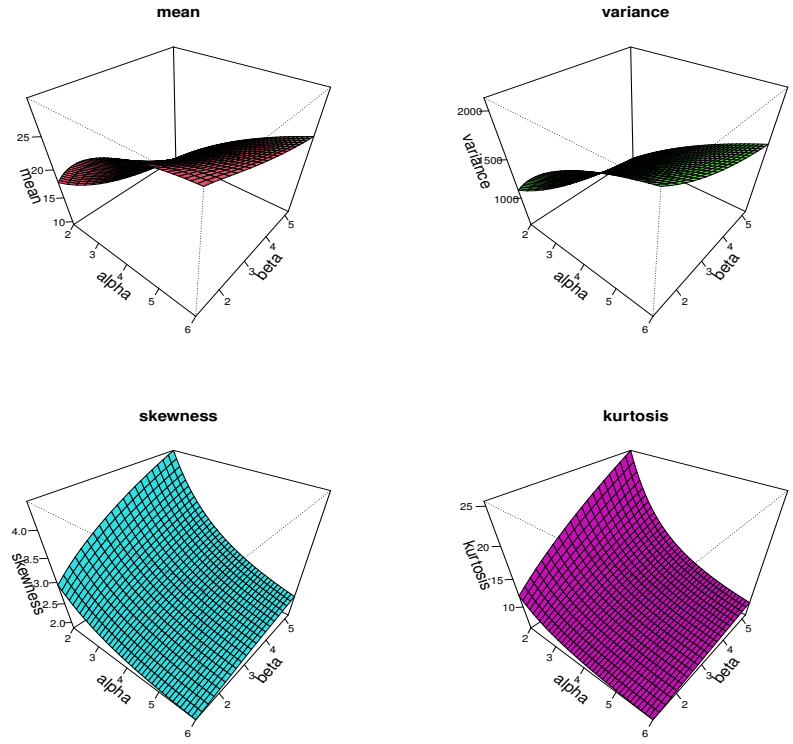


Figure 3: Moments for the MAPTLo distribution at $\theta = 0.6$.

Additionally, the incomplete moments (IMs) and conditional moments (CMs) of the MAPTLo

distribution are, respectively, given by

$$\begin{aligned} E(Y^r|Y \le t) = \phi_r(t) &= \int_0^t y^r f(y;\alpha,\beta,\theta)dy \\ &= \sum_{s=0}^{\infty}\sum_{k=0}^{s} \Upsilon_{s,k} \int_0^t y^r g(y;\beta,(1+k)\theta)dy \\ &= \sum_{s=0}^{\infty}\sum_{k=0}^{s} \Upsilon_{s,k} \int_0^t y^r \beta(1+k)\theta(1+\beta y)^{-(1+k)\theta-1}dy \\ &= \sum_{s=0}^{\infty}\sum_{k=0}^{s} \Upsilon_{s,k} \frac{(1+k)t^{r+1}\beta\theta * 2F1[r+1,(1+k)\theta+1;r+2;-t\beta]}{r+1}, \end{aligned} \tag{16}$$

and

$$E(Y^r|Y > t) = \frac{1}{R(t)}\int_t^{\infty} y^r f(y;\alpha,\beta,\theta)dy = \frac{1}{R(t)}(E(Y^r) - \phi_r(t)). \tag{17}$$

3.3 Lorenz and Bonferroni curves

The Lorenz and Bonferroni curves have found applications in sundry fields, such as economics. The Lorenz curve of the MAPTLo distribution is

$$L(q) = \frac{1}{\mu}\int_0^p yf(y)dy = \frac{1}{\mu}\sum_{s=0}^{\infty}\sum_{k=0}^{s}\Upsilon_{s,k}\frac{(1+\beta p)^{-(1+k)\theta}\left[-1+(1+\beta p)^{(1+k)\theta}-(1+k)p\beta\theta\right]}{\beta((1+k)\theta-1)}, \tag{18}$$

and the Bonferroni curve of MAPTLo distribution is

$$B(q) = \frac{1}{q\mu}\int_0^p yf(y)dy = \frac{1}{q\mu}\sum_{s=0}^{\infty}\sum_{k=0}^{s}\Upsilon_{s,k}\frac{(1+\beta p)^{-(1+k)\theta}\left[-1+(1+\beta p)^{(1+k)\theta}-(1+k)p\beta\theta\right]}{\beta((1+k)\theta-1)}, \tag{19}$$

where $p = Q_{MAPTLo}(q)$ is the quantile function of Y at q and $\mu = E(Y)$. The behaviors of Lorenz and Bonferroni curves can be easily viewed through Figure 4.

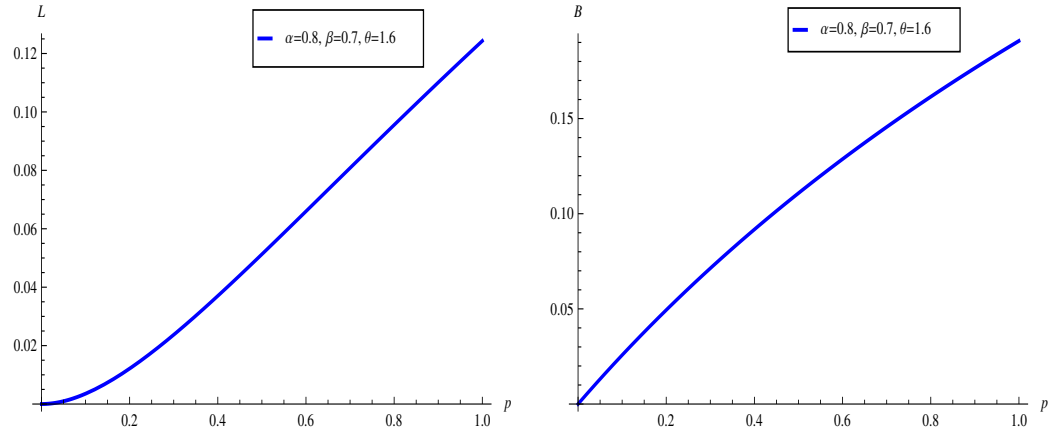


Figure 4: Shapes of the Lorenz curve (left) and the Bonferroni curve (right) of the MAPTLo.

3.4 Entropies

The entropy is widely used in a variety of physical, medical and biological applications.

3.4 Rényi entropy

The Rényi entropy [34] with $\delta > 0$, $\delta \neq 1$ for the MAPTLo distribution can be formulated as

$$
\begin{aligned}
H_\delta &= \frac{1}{1-\delta}\log\left(\int_0^\infty (f(y))^\delta dy\right)\\
&= \frac{1}{1-\delta}\log\left\{\left(\frac{\alpha\beta\theta\log\alpha}{\alpha-1}\right)^\delta \int_0^\infty \left[\frac{(1+\beta y)^{-\theta-1}\alpha^{1-(1+\beta y)^{-\theta}}}{(1+\alpha-\alpha^{1-(1+\beta y)^{-\theta}})^2}\right]^\delta dy\right\}\\
&= \frac{1}{1-\delta}\log\left\{\left(\frac{\alpha\beta\theta\log\alpha}{\alpha-1}\right)^\delta \sum_{j,s=0}^{\infty}\sum_{b=0}^{s}\frac{(-1)^b((\delta+j)\log\alpha)^s\binom{s}{b}\Gamma(2\delta+j)}{(\alpha+1)^{2\delta+j}s!\Gamma(2\delta)j!}\right.\\
&\left.\times\int_0^\infty (1+\beta y)^{-[(\delta+b)\theta+\delta]}dy\right\}\\
&= \frac{1}{1-\delta}\log\left\{\left(\frac{\alpha\beta\theta\log\alpha}{\alpha-1}\right)^\delta \sum_{j,s=0}^{\infty}\sum_{b=0}^{s}\frac{(-1)^b((\delta+j)\log\alpha)^s\binom{s}{b}\Gamma(2\delta+j)}{(\alpha+1)^{2\delta+j}s!\Gamma(2\delta)j!}\right.\\
&\left.\times\frac{1}{\beta[(\delta+b)\theta+\delta-1]}\right\}, \qquad (\delta+b)\theta+\delta>1.
\end{aligned}
\tag{20}
$$

3.4 Tsallis entropy

The Tsallis entropy [35] with $\delta > 0$, $\delta \neq 1$ for the MAPTLo distribution can be formulated as

$$
\begin{aligned}
TS_\delta &= \frac{1}{\delta-1}\left(1-\int_0^\infty (f_{MAPTLo}(y;\alpha,\beta,\theta))^\delta dy\right)\\
&= \frac{1}{\delta-1}\left\{1-\left(\frac{\alpha\beta\theta\log\alpha}{\alpha-1}\right)^\delta \sum_{j,s=0}^{\infty}\sum_{b=0}^{s}\frac{(-1)^b((\delta+j)\log\alpha)^s\binom{s}{b}\Gamma(2\delta+j)}{(\alpha+1)^{2\delta+j}s!\Gamma(2\delta)j!}\right.\\
&\left.\times\frac{1}{\beta[(\delta+b)\theta+\delta-1]}\right\}, \qquad (\delta+b)\theta+\delta>1.
\end{aligned}
\tag{21}
$$

The behaviors of the Rényi and Tsallis entropies can be easily viewed through Figures 5 and 6.

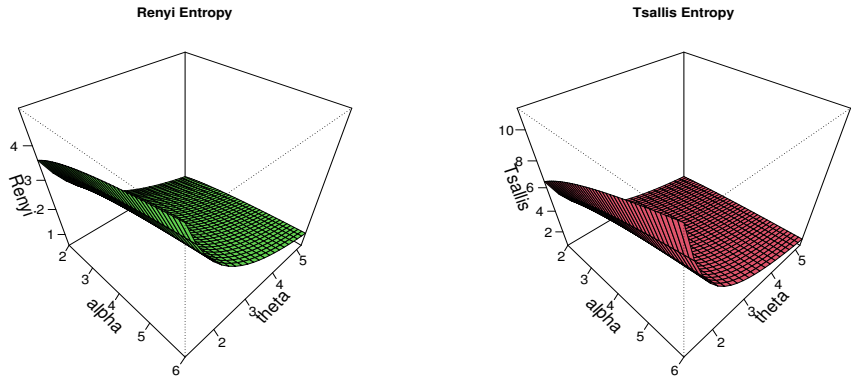


Figure 5: Entropies for the MAPTLo distribution at $\beta = 0.8$.

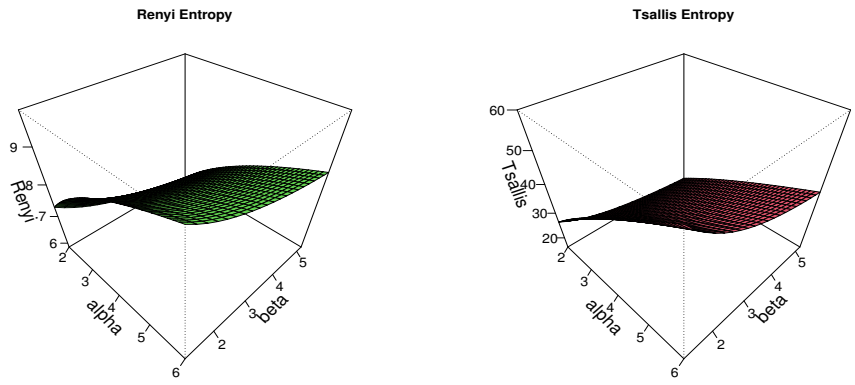


Figure 6: Entropies for the MAPTLo distribution at $\theta = 0.6$.

Table 1 gives the entropies of the MAPTLo distribution for various values of the parameters.

Table 1: Entropies of MAPTLo with various values of parameters.

δ	α	β	θ	H_δ	TS_δ
0.7	0.6	0.5	0.8	3.75326	6.94411
			1.1	2.70669	4.17476
		1.2	0.8	2.87779	4.57019
			1.1	1.83123	2.44052
	1.3	0.5	0.8	5.12993	12.1995
			1.1	3.79799	7.08296
		1.2	0.8	4.25447	8.61166
			1.1	2.92252	4.67698
1.6	0.6	0.5	0.8	1.53154	1.00175
			1.1	1.12538	0.81827
		1.2	0.8	0.65607	0.54234
			1.1	0.24993	0.23209
	1.3	0.5	0.8	2.76608	1.34966
			1.1	2.25067	1.23478
		1.2	0.8	1.89061	1.13062
			1.1	1.37523	0.93637

From Table 1, one can observe the following:

- If α is increasing (β and θ are fixed), then the entropies are increasing.
- If β is increasing (α and θ are fixed), then the entropies are decreasing.
- If θ is increasing (α and β are fixed), then the entropies are decreasing.

3.5 Order statistics

Let $Y_1, \ldots, Y_n$ be a random sample from the MAPTLo distribution, and let $Y_{1:n}, \ldots, Y_{n:n}$ be the order statistics of the random sample. Therefore, the PDF of the j^{th} order statistic $Y_{j:n}$ can be formulated as

$$
\begin{aligned}
f_{j:n}(y) &= \frac{n!}{(n-j)!(j-1)!} f(y)[F(y)]^{j-1}[1-F(y)]^{n-j} \\
&= \frac{n!}{(n-j)!(j-1)!} f(y) \sum_{c=0}^{n-j} (-1)^c \binom{n-j}{c} [F(y)]^{c+j-1} \\
&= \frac{n!}{(n-j)!(j-1)!} \sum_{c=0}^{n-j} (-1)^c \binom{n-j}{c} \left[\frac{\alpha\beta\theta \log(\alpha)(1+\beta y)^{-(\theta+1)} \alpha^{1-(1+\beta y)^{-\theta}}}{(\alpha-1)(\alpha+1)^2 (1-\frac{\alpha^{1-(1+\beta y)^{-\theta}}}{\alpha+1})^2} \right] \\
&\times \left[\frac{\alpha^{1-(1+\beta y)^{-\theta}} - 1}{(\alpha-1)(\alpha+1)(1-\frac{\alpha^{1-(1+\beta y)^{-\theta}}}{\alpha+1})} \right]^{c+j-1} \\
&= \frac{n!}{(n-j)!(j-1)!} \sum_{c=0}^{n-j} (-1)^{j-1} \binom{n-j}{c} \left[\frac{\alpha\beta\theta \log(\alpha)(1+\beta y)^{-(\theta+1)}}{(\alpha-1)^{c+j}(\alpha+1)^{c+j+1}} \right] \\
&\times \alpha^{1-(1+\beta y)^{-\theta}} (1-\alpha^{1-(1+\beta y)^{-\theta}})^{c+j+1} (1-\frac{\alpha^{1-(1+\beta y)^{-\theta}}}{\alpha+1})^{-(c+j+1)} \\
&= \frac{n!}{(n-j)!(j-1)!} \sum_{c=0}^{n-j} \sum_{s=0}^{c+j-1} \sum_{b,k}^{\infty} \sum_{m=0}^{k} (-1)^{j+m+s-1} \binom{n-j}{c} \binom{c+j-1}{s} \binom{k}{m} \\
&\times \frac{\Gamma(b+c+j+1)(b+s+1)^k (\log\alpha)^{1+k} \alpha}{\Gamma(c+j+1) b! (\alpha-1)^{c+j} (\alpha+1)^{b+c+j+1} k!(1+m)} (1+m)\beta\theta(1+\beta y)^{-(1+m)\theta-1} \\
&= \sum_{k=0}^{\infty} \sum_{m=0}^{k} \Upsilon_{k,m} g(y;\beta,(1+m)\theta), \qquad (22)
\end{aligned}
$$

where $g(y;\beta,(1+m)\theta)$ is the PDF of the Lo distribution with parameters β and $(1+m)\theta$ and

$$
\begin{aligned}
\Upsilon_{k,m} &= \frac{n!}{(n-j)!(j-1)!} \sum_{c=0}^{n-j} \sum_{s=0}^{c+j-1} \sum_{b=0}^{\infty} \frac{(-1)^{j+m+s-1} \alpha (\log\alpha)^{1+k} (b+s+1)^k \Gamma(b+c+j+1)}{(\alpha-1)^{c+j}(\alpha+1)^{b+c+j+1}(1+m) b! k! \Gamma(c+j+1)} \\
&\times \binom{n-j}{c} \binom{c+j-1}{s} \binom{k}{m}.
\end{aligned}
$$

The r^{th} moments of $Y_{j:n}$ may be calculated as follows using Eq.(22)

$$
E(Y_{j:n}^r) = \int_0^{\infty} y^r f_{j:n}(y) dy = \sum_{k=0}^{\infty} \sum_{m=0}^{k} \Upsilon_{k,m} \frac{r! \Gamma((1+m)\theta - r)}{\beta^r \Gamma((1+m)\theta)}, \qquad (1+m)\theta > r. \qquad (23)
$$

4 Reliability functions

The reliability function (RF) of the MAPTLo distribution is described as

$$
\begin{aligned}
R_{MAPTLo}(y) &= 1 - \frac{\alpha^{1-(1+\beta y)^{-\theta}} - 1}{(\alpha-1)(1+\alpha-\alpha^{1-(1+\beta y)^{-\theta}})} \\
&= \frac{\alpha(\alpha-\alpha^{1-(1+\beta y)^{-\theta}})}{(\alpha-1)(1+\alpha-\alpha^{1-(1+\beta y)^{-\theta}})}. \qquad (24)
\end{aligned}
$$

The hazard rate function (HRF) of the MAPTLo distribution can be formulated as

$$
h_{MAPTLo}(y) = \frac{f(y)}{R(y)} = \frac{\beta\theta(1+\beta y)^{-(\theta+1)} \alpha^{1-(1+\beta y)^{-\theta}} \log(\alpha)}{(1+\alpha-\alpha^{1-(1+\beta y)^{-\theta}})(\alpha-\alpha^{1-(1+\beta y)^{-\theta}})}. \qquad (25)
$$

Figure 7 includes several types of HRF shapes. It shows that Figure (a) is decreasing, Figure (b) is increasing, and Figure (c) is unimodal.

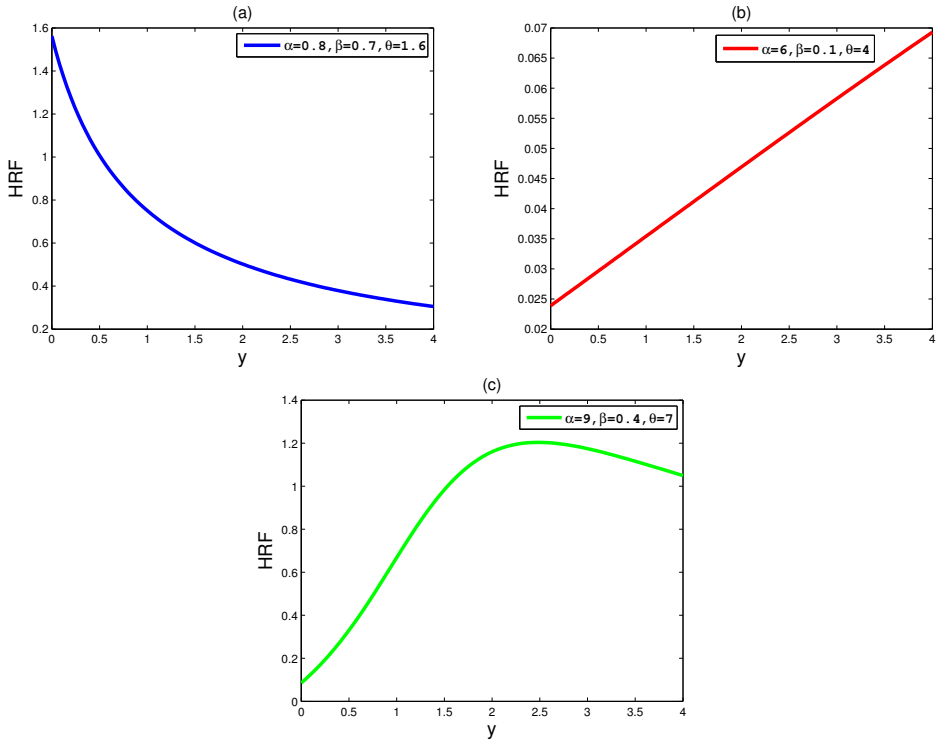


Figure 7: Some shapes of HRF.

The reversed hazard rate (RHR) function of the MAPTLo distribution is described as

$$r_{MAPTLo}(y) = \frac{f(y)}{F(y)} = \frac{\alpha\beta\theta(1+\beta y)^{-(\theta+1)}\alpha^{1-(1+\beta y)^{-\theta}}\log(\alpha)}{(1+\alpha-\alpha^{1-(1+\beta y)^{-\theta}})(-1+\alpha^{1-(1+\beta y)^{-\theta}})}. \tag{26}$$

4.1 Mean residual life

The mean residual life (MRL) function of the MAPTLo distribution is described as

$$\begin{aligned}\mu(t) = E(Y-t|Y>t) &= \frac{1}{R(t)}\int_t^{\infty}(y-t)f(y)dy \\ &= \frac{1}{R(t)}\left(1-\int_0^t yf(y)dy\right)-t \\ &= \frac{(\alpha-1)(1+\alpha-\alpha^{1-(1+\beta t)^{-\theta}})}{\alpha(\alpha-\alpha^{1-(1+\beta t)^{-\theta}})}\Big(1-\phi_1(t)\Big)-t,\end{aligned} \tag{27}$$

where

$$\phi_1(t) = \sum_{s=0}^{\infty}\sum_{k=0}^{s}\Upsilon_{s,k}\frac{(1+\beta t)^{-(1+k)\theta}\Big[-1+(1+\beta t)^{(1+k)\theta}-(1+k)t\beta\theta\Big]}{\beta((1+k)\theta-1)}.$$

Figure 8 includes several MRL shapes. From Figure 7 of the HRF and Figure 8 of the MRL, we conclude that if the HRF is decreasing, then the MRL is increasing for the same parameter values.

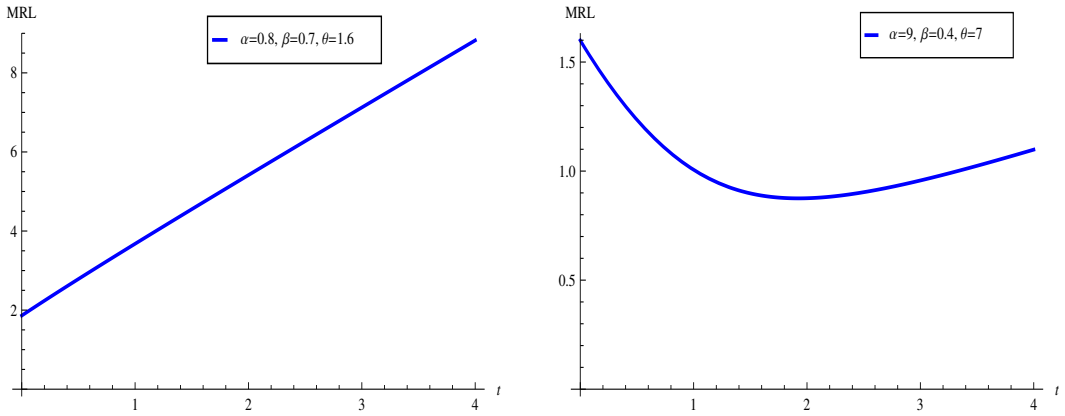


Figure 8: Different shapes of MRL.

4.2 Mean inactivity time

The mean inactivity time (MIT) function of the MAPTLo distribution is described as

$$m(t) = E(t - Y|Y \leq t) = t - \frac{1}{F(t)} \int_0^t y f(y) dy = t - \frac{\phi_1(t)}{F(t)}$$

$$= t - \frac{(\alpha - 1)(1 + \alpha - \alpha^{1-(1+\beta t)^{-\theta}})}{\alpha^{1-(1+\beta t)^{-\theta}} - 1} \phi_1(t), \qquad t > 0. \tag{28}$$

Figure 9 includes graphs of the RHR and MIT. From Figure 9, we conclude that if the RHR is decreasing, then the MIT is increasing for the same parameter values.

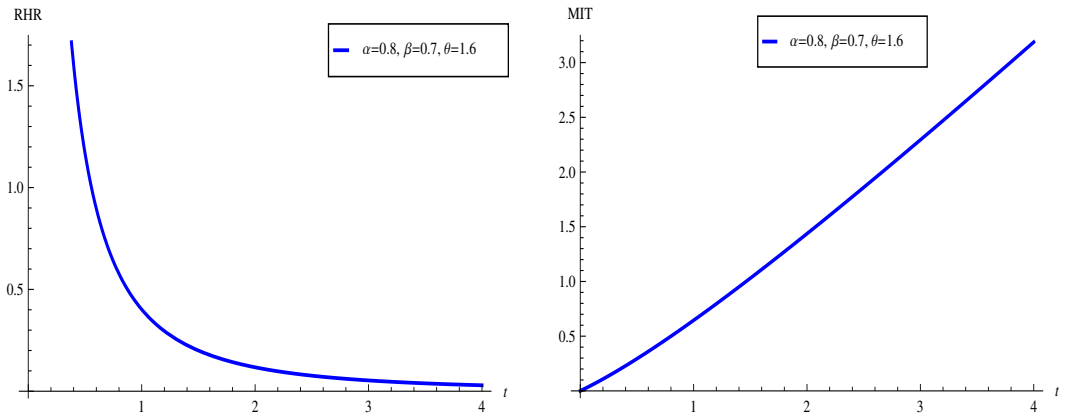


Figure 9: Shapes of the RHR (left) and the MIT (right) of the MAPTLo.

4.3 Stress-Strength reliability

Let Z_1 and Z_2 describe the stress and strength, respectively, and let $Z_1 \sim \text{MAPTLo}(\alpha_1, \beta_1, \theta_1)$ and $Z_2 \sim \text{MAPTLo}(\alpha_2, \beta_2, \theta_2)$. Therefore, the stress-strength reliability R is derived as

$$R = P(Z_2 > Z_1) = \int_0^\infty F_1(z) f_2(z) dz$$

$$= \int_0^\infty \left[\frac{\alpha_1^{1-(1+\beta_1 z)^{-\theta_1}} - 1}{(\alpha_1 - 1)(1 + \alpha_1 - \alpha_1^{1-(1+\beta_1 z)^{-\theta_1}})} \right] \left[\frac{\alpha_2 \beta_2 \theta_2 \log(\alpha_2)(1 + \beta_2 z)^{-(\theta_2+1)} \alpha_2^{1-(1+\beta_2 z)^{-\theta_2}}}{(\alpha_2 - 1)(1 + \alpha_2 - \alpha_2^{1-(1+\beta_2 z)^{-\theta_2}})^2} \right] dz$$

AdvantaCore Scientific Publishing

$$= \frac{\alpha_2\beta_2\theta_2\log(\alpha_2)}{(\alpha_1-1)(\alpha_2-1)(\alpha_1+1)(\alpha_2+1)^2}\int_0^\infty (1+\beta_2 z)^{-(\theta_2+1)}(\alpha_1^{1-(1+\beta_1 z)^{-\theta_1}}-1)\alpha_2^{1-(1+\beta_2 z)^{-\theta_2}}$$

$$\times\left(1-\frac{\alpha_1^{1-(1+\beta_1 z)^{-\theta_1}}}{\alpha_1+1}\right)^{-1}\left(1-\frac{\alpha_2^{1-(1+\beta_2 z)^{-\theta_2}}}{\alpha_2+1}\right)^{-2}dz$$

$$= \frac{\alpha_2\beta_2\theta_2\log(\alpha_2)}{(\alpha_1-1)(\alpha_2-1)(\alpha_1+1)(\alpha_2+1)^2}\int_0^\infty (1+\beta_2 z)^{-(\theta_2+1)}(\alpha_1^{1-(1+\beta_1 z)^{-\theta_1}}-1)\alpha_2^{1-(1+\beta_2 z)^{-\theta_2}}$$

$$\times\left(\sum_{j_1=0}^{\infty}\frac{\alpha_1^{j_1(1-(1+\beta_1 z)^{-\theta_1})}}{(\alpha_1+1)^{j_1}}\right)\left(\sum_{j_2=0}^{\infty}(j_2+1)\frac{\alpha_2^{j_2(1-(1+\beta_2 z)^{-\theta_2})}}{(\alpha_2+1)^{j_2}}\right)dz$$

$$= \frac{\alpha_2\beta_2\theta_2}{(\alpha_1-1)(\alpha_2-1)}\sum_{j_1,j_2=0}^{\infty}\sum_{k_1,k_2=0}^{\infty}\sum_{s_1=0}^{k_1}\sum_{s_2=0}^{k_2}\Psi_{j_1,j_2}\Psi_{k_1,k_2}\Psi_{s_1,s_2}\int_0^\infty (1+\beta_1 z)^{-s_1\theta_1}(1+\beta_2 z)^{-(s_2+1)\theta_2-1}dz,$$

where

$$\Psi_{j_1,j_2} = \frac{(j_2+1)^{1+k_2}}{(\alpha_1+1)^{1+j_1}(\alpha_2+1)^{2+j_2}},\ \Psi_{k_1,k_2} = \frac{(\log\alpha_1)^{k_1}(\log\alpha_2)^{1+k_2}}{k_1!k_2!},\ \text{and}\ \Psi_{s_1,s_2} = (-1)^{s_1+s_2}\binom{k_1}{s_1}\binom{k_2}{s_2}.$$

5 Parameter estimation

Within this part, the maximum likelihood technique is utilized to estimate the different parameters of the MAPTLo distribution.

5.1 Maximum likelihood estimation

Here, we discuss the MLE for the different parameters $\underline{\Theta} = (\alpha, \beta, \theta)^\top$ of the MAPTLo distribution using Eq. (8) of the PDF. Let $y_1, y_2, ..., y_n$ be a complete random sample of size n from the MAPTLo distribution. The logarithm of the likelihood function can be formulated as

$$L(y_1,...,y_n|\underline{\Theta}) = n\log\left(\frac{\alpha\beta\theta\log(\alpha)}{\alpha-1}\right) - (\theta+1)\sum_{i=1}^{n}\log(1+\beta y_i)$$
$$+\log(\alpha)\sum_{i=1}^{n}(1-(1+\beta y_i)^{-\theta}) - 2\sum_{i=1}^{n}\log(1+\alpha-\alpha^{1-(1+\beta y_i)^{-\theta}}), \tag{29}$$

The three first partial derivatives of Eq. (29) with respect to the parameters are, respectively, expressed by

$$\frac{\partial L}{\partial\alpha} = \frac{n}{\alpha}+\frac{n}{\alpha\log(\alpha)}-\frac{n}{\alpha-1}+\frac{1}{\alpha}\sum_{i=1}^{n}(1-(1+\beta y_i)^{-\theta}) - 2\sum_{i=1}^{n}\frac{1-[1-(1+\beta y_i)^{-\theta}]\alpha^{-(1+\beta y_i)^{-\theta}}}{1+\alpha-\alpha^{1-(1+\beta y_i)^{-\theta}}},$$

$$\frac{\partial L}{\partial\beta} = \frac{n}{\beta}-\sum_{i=1}^{n}\frac{(\theta+1)y_i}{1+\beta y_i}+\log(\alpha)\sum_{i=1}^{n}\theta y_i(1+\beta y_i)^{-(\theta+1)}+\sum_{i=1}^{n}\frac{2\theta\log(\alpha)y_i(1+\beta y_i)^{-(\theta+1)}\alpha^{1-(1+\beta y_i)^{-\theta}}}{1+\alpha-\alpha^{1-(1+\beta y_i)^{-\theta}}},$$

and

$$\frac{\partial L}{\partial \theta} = \frac{n}{\theta} - \sum_{i=1}^{n} \log(1+\beta y_i) + \log(\alpha) \sum_{i=1}^{n} (1+\beta y_i)^{-\theta} \log(1+\beta y_i)$$

$$+ 2 \sum_{i=1}^{n} \frac{\log(\alpha)(1+\beta y_i)^{-\theta} \log(1+\beta y_i) \alpha^{1-(1+\beta y_i)^{-\theta}}}{1+\alpha-\alpha^{1-(1+\beta y_i)^{-\theta}}}.$$

We can use any program to obtain the MLEs of $\underline{\Theta}$ in order to solve the above three normal equations.

5.2 Simulation

In this subsection, we examine the behavior of the MLEs derived from unknown parameters. The simulation was carried out using Mathematica version 10. Six different sets of initial parameter values are considered, and the simulation results are based on sample sizes n (= 40, 90, 140, 190, 240, 300). The simulation study is implemented using the steps below:

1. Establish the sample size and initial parameter values.
2. Create a random sample of size n from the MAPTLo distribution using Eq. (12).
3. Compute the mean squared error (MSE) of the parameters.
4. Compute the bias of the parameters.
5. Repeat Steps 2–4 10000 times.
6. The MSE and bias of the respective estimators are given by

$$\text{MSE}(\hat{\Theta}) = \frac{1}{10000} \sum_{i=1}^{10000} (\hat{\Theta}_i - \Theta)^2, \quad \text{Bias}(\hat{\Theta}) = \frac{1}{10000} \sum_{i=1}^{10000} (\hat{\Theta}_i - \Theta), \tag{30}$$

where $\hat{\Theta} = (\hat{\alpha}, \hat{\beta}, \hat{\theta})^\top$. Table 2 shows the MSE and bias of $\hat{\alpha}$, $\hat{\beta}$, and $\hat{\theta}$. From Table 2, one can observe that the MSE and bias for the MLEs of α, β, and θ decrease as n increases.

Table 2: Simulation results for MLEs.

MAPTLo(α, β, θ)	n	MSE$(\hat{\alpha})$	Bias$(\hat{\alpha})$	MSE$(\hat{\beta})$	Bias$(\hat{\beta})$	MSE$(\hat{\theta})$	Bias$(\hat{\theta})$
	40	0.15645	0.02813	0.08188	0.06737	0.12356	0.21669
(0.3, 0.1, 0.2)	90	0.10097	0.02609	0.03308	0.03398	0.07773	0.15161
	140	0.06883	0.02466	0.01486	0.02146	0.05331	0.11056
	190	0.04989	0.02295	0.00896	0.01452	0.04042	0.08665
	240	0.03703	0.02204	0.00511	0.01098	0.02948	0.06534
	300	0.02878	0.01855	0.00386	0.00886	0.02386	0.05452
	40	0.13812	0.08114	0.14398	0.07329	0.1597	0.24911
(0.2, 0.2, 0.2)	90	0.09366	0.06232	0.09546	0.06323	0.1006	0.17753
	140	0.06752	0.05145	0.06813	0.05368	0.0788	0.14792
	190	0.04329	0.03969	0.04032	0.03797	0.0613	0.11848
	240	0.03504	0.03572	0.03102	0.03367	0.0505	0.09937
	300	0.02449	0.02811	0.02198	0.02675	0.0397	0.07987
	40	0.36708	-0.10751	2.02246	-1.33021	0.09352	0.11972
(0.5, 1.6, 0.8)	90	0.29399	0.07469	1.94375	-1.28285	0.06162	0.08556
	140	0.11798	0.04405	1.91874	-1.27156	0.04611	0.06443
	190	0.10451	0.02832	1.87831	-1.24984	0.04022	0.05178
	240	0.07451	0.01726	1.46254	-1.20348	0.03816	0.04624
	300	0.05029	-0.00847	1.29382	-0.79357	0.02856	0.03645

Table 2: Simulation results for MLEs (continued).

MAPTLo(α,β,θ)	n	MSE$(\hat{\alpha})$	Bias$(\hat{\alpha})$	MSE$(\hat{\beta})$	Bias$(\hat{\beta})$	MSE$(\hat{\theta})$	Bias$(\hat{\theta})$
	40	0.20171	-0.04431	0.15231	0.05861	0.12087	0.21045
(0.4, 0.2, 0.3)	90	0.15816	-0.02141	0.10572	0.05062	0.07724	0.15004
	140	0.12697	-0.00901	0.07656	0.04625	0.05792	0.12075
	190	0.10355	0.00471	0.05519	0.03658	0.04675	0.10122
	240	0.07946	-0.00438	0.03720	0.02585	0.04184	0.09339
	300	0.06273	0.00058	0.02678	0.02159	0.03228	0.07349
	40	1.60882	-1.15333	0.25124	-0.27267	0.28961	-0.26884
(1.5, 0.5, 1.4)	90	1.48695	-1.07258	0.24996	-0.18136	0.23621	-0.20129
	140	1.39951	-1.00941	0.24836	-0.13331	0.19729	-0.15534
	190	1.32861	-0.96758	0.24572	-0.09365	0.16868	-0.12000
	240	1.28128	-0.92955	0.24421	-0.07337	0.15622	-0.10503
	300	1.21952	-0.89057	0.24395	-0.03906	0.13731	-0.08088
	40	0.17071	0.15582	0.13784	0.12017	0.24139	0.31787
(0.1, 0.1, 0.2)	90	0.15246	0.13953	0.12391	0.11726	0.14037	0.21329
	140	0.10745	0.10543	0.09119	0.09227	0.10191	0.17205
	190	0.08077	0.08247	0.06487	0.06935	0.08451	0.14592
	240	0.06039	0.06616	0.04887	0.05467	0.07015	0.12405
	300	0.04059	0.05369	0.03439	0.04341	0.06093	0.11072

6 Real data

To demonstrate the efficacy of the MAPTLo distribution, three different application datasets are used, highlighting that the MAPTLo distribution can serve as a robust lifetime distribution compared to more widely known distributions, such as the APTLo, APT inverse Lo (APTILo), APT inverse Lindley (APTIL), inverse Lo (ILo), and inverse Lindley (IL) distributions. The PDFs of these competitive distributions are listed as

- APTLo: $f(y;\alpha,\beta,\theta) = \frac{\alpha\beta\theta\log(\alpha)(1+\beta y)^{-(\theta+1)}\alpha^{1-(1+\beta y)^{-\theta}}}{(\alpha-1)}, \quad y>0,\alpha,\beta,\theta>0.$
- APTILo: $f(y;\alpha,\beta,\theta) = \frac{\log(\alpha)}{\alpha-1}(\frac{\beta\theta}{y^2})(1+\frac{\beta}{y})^{-(\theta+1)}\alpha^{(1+\frac{\beta}{y})^{-\theta}}, \quad y>0,\alpha,\beta,\theta>0.$
- APTIL: $f(y;\alpha,\theta) = \frac{\log(\alpha)}{\alpha-1}(\frac{\theta^2}{\theta+1})(\frac{y+1}{y^3})e^{-\frac{\theta}{y}}\alpha^{[1+\frac{\theta}{(\theta+1)y}]e^{-\frac{\theta}{y}}}, \quad y>0,\alpha>0,\theta>0.$
- ILo: $f(y;\beta,\theta) = (\frac{\beta\theta}{y^2})(1+\frac{\beta}{y})^{-(\theta+1)}, \quad y>0,\beta>0,\theta>0.$
- IL: $f(y;\theta) = \frac{\theta^2}{\theta+1}(\frac{y+1}{y^3})e^{-\frac{\theta}{y}}; \quad y>0,\theta>0.$

The first dataset pertains to COVID-19 statistics specific to the Netherlands, encompassing a duration of 30 days, with recordings spanning from 31 March to 30 April 2020. This dataset is characterized by a crude mortality rate. The second dataset comprises the failure times of a sample consisting of 25 devices subjected to a temperature of 180°C, as elucidated by Pham [36]. The third dataset delineates the mortality rates attributable to the COVID-19 pandemic within the United Kingdom over a period of 76 days, specifically from 15 April to 30 June 2020. This dataset was originally examined by Mubarak et al. [37]. All datasets are presented in Table 3.

Table 3: Real Datasets.

First data	14.918	10.656	12.274	10.289	10.832	7.099	5.928	13.211
	7.968	7.584	5.555	6.027	4.097	3.611	4.960	7.498
	6.940	5.307	5.048	2.857	2.254	5.431	4.462	3.883
	3.461	3.647	1.974	1.273	1.416	4.235		

Table 3: Real Datasets (continued).

Second data	112	260	298	327	379	487	593	658
	701	720	734	736	775	915	974	1023
	1157	1227	1293	1335	1472	1529	1545	2029
	4568							
Third data	0.0587	0.0863	0.1165	0.1247	0.1277	0.1303	0.1652	0.2079
	0.2395	0.2751	0.2845	0.2992	0.3188	0.3317	0.3446	0.3553
	0.3622	0.3926	0.3926	0.4110	0.4633	0.4690	0.4954	0.5139
	1.0438	1.0602	1.1305	1.1468	0.5696	0.5837	0.6197	0.6365
	0.7096	0.7193	0.7444	0.8590	1.1533	1.2260	1.2707	1.3423
	1.4149	1.5709	1.6017	1.6083	1.6324	1.6998	1.8164	1.8392
	1.8721	1.9844	2.1360	2.3987	2.4153	2.5225	2.7087	2.7946
	3.3609	3.3715	3.7840	3.9042	4.1969	4.3451	4.4627	4.6477
	5.3664	5.4500	5.7522	6.4241	7.0657	7.4456	8.2307	9.6315
	10.187	11.1429	11.2019	11.4584				

The descriptive analyses are presented in Table 4.

Table 4: Summary statistics for the selected datasets.

Data	Mean	Std. deviation	Q_1	Median	Q_3	Skewness	Kurtosis
First Data	6.1565	3.5333	3.647	5.307	7.584	0.833971	2.9534
Second Data	1037.88	876.13	593	775	1293	2.69223	11.673
Third Data	2.43719	2.9359	0.3926	1.226	3.3609	1.7026	5.0908

Before discussing all datasets, we first present the corresponding TTT plots. Figure 10 illustrates the TTT plots for all datasets. It shows that the TTT plots for the first and second datasets are concave, while the third dataset is convex. The box plots for the sundry datasets are displayed in Figure 11. It shows that the first dataset is approximately symmetric, while the second and third datasets are positively skewed.

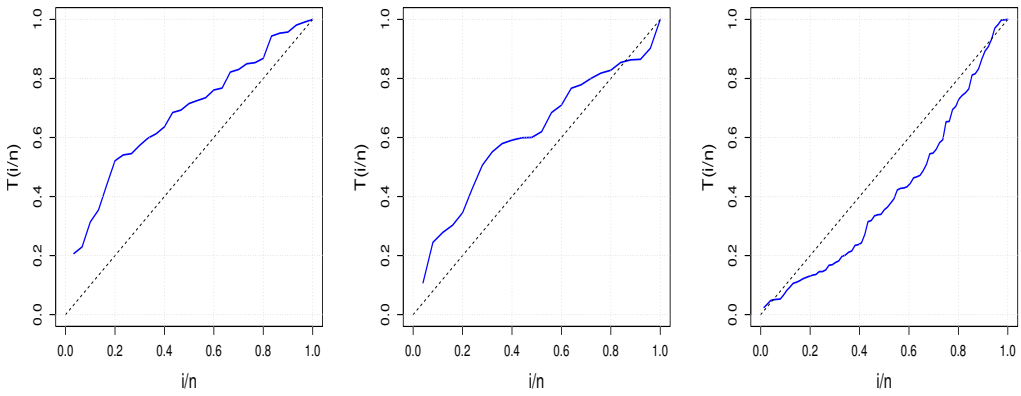


Figure 10: TTT plots for first data (left), second data (center) and third data (right).

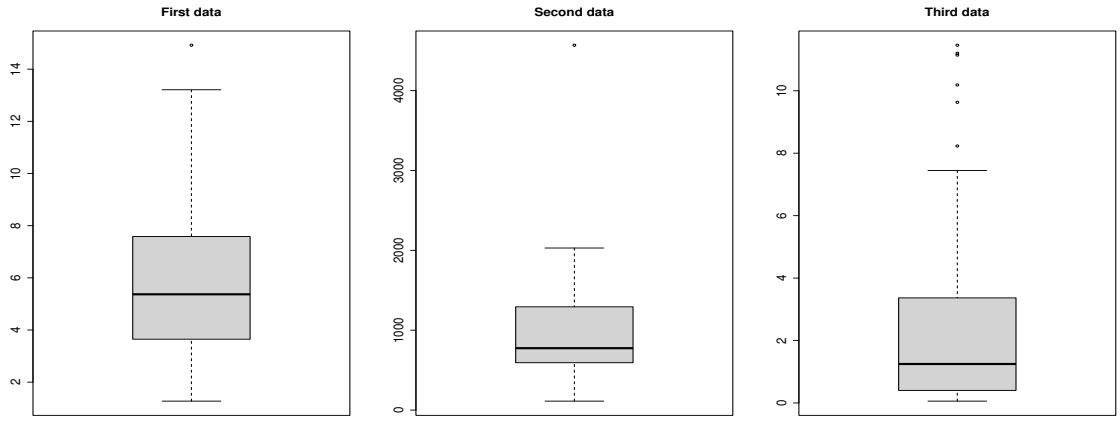


Figure 11: Box plot of all data.

The MLEs of the MAPTLo distribution, along with those of other competitive distributions, are presented in Tables 5–7 for all datasets. Additionally, goodness-of-fit statistics, including the Akaike information criterion (AIC) Akaike [38], Bayesian information criterion (BIC) Schwarz [39], Cramér-von Mises (CM), Anderson-Darling (AD), and Kolmogorov-Smirnov (K-S) test with p-values, are also provided in these tables. It shows that the MAPTLo distribution has the smallest values of AIC, BIC, CM, AD, and K-S, along with the highest p-value. From the results shown in these tables, it is evident that the MAPTLo distribution outperforms the other competitive distributions. Consequently, the MAPTLo distribution is identified as the best model for fitting the given datasets. In addition, by using the observed Fisher information matrix, the approximate 95% two sided confidence intervals (CIs) of the unknown parameters α, β and θ are given in Table 8. Figures 12–14 illustrate the fitted RFs, PDFs, P-P plots, and Q-Q plots (the Q–Q plot is used to check the validity of the distributional assumption for the data) for the MAPTLo distribution across all datasets. It can be seen from Figures 12–14 that the graphical presentations support the same numerical findings presented in Tables 5–7, respectively. Thus, the proposed MAPTLo distribution provides the best fit for the given datasets.

Table 5: MLEs and different statistics of the MAPTLo distribution and other models for the first dataset.

Model	Parameters	-2L	AIC	BIC	CM	AD	K-S	p-value
MAPTLo	α=34.415 β=0.381 θ=4.275	154.592	160.592	161.937	0.0352	0.1777	0.0781	0.993
APTLo	α=651.935 β=0.042 θ=10.931	156.082	162.082	166.285	0.0339	0.1673	0.0798	0.991
APTILo	α=423.593 β=0.269 θ=2.741	175.009	181.009	185.212	0.0677	0.4084	0.2523	0.044
APTIL	α=0.0085 θ=10.302	159.979	163.979	166.782	0.1103	0.6835	0.1112	0.852
Lo	β=0.093 θ=1.959	179.022	183.022	185.824	0.0378	0.1976	0.2548	0.041
ILo	β=0.129 θ=33.278	171.324	175.324	178.126	0.0972	0.5945	0.2496	0.048
IL	θ=4.959	170.475	172.475	173.876	0.1071	0.6552	0.2428	0.058

Table 6: MLEs and different statistics of the MAPTLo distribution and other models for the second dataset.

Model	Parameters	-2L	AIC	BIC	CM	AD	K-S	p-value
MAPTLo	α=120.92	389.405	395.405	399.061	0.056	0.253	0.1005	0.962
	β=0.0127							
	θ=2.601							
APTLo	α=34.956	404.453	410.453	414.11	0.0814	0.3916	0.2581	0.0716
	β=0.00477							
	θ=1.0302							
APTILo	α=11826.4	399.94	405.94	409.60	0.1136	0.6681	0.2532	0.066
	β=0.0146							
	θ=4661.4							
APTIL	α=7912910	399.685	403.685	406.122	0.1424	0.7387	0.245	0.097
	θ=39.806							
Lo	β=0.0023	415.69	419.69	422.13	0.08601	0.4195	0.283	0.0356
	θ=0.6745							
ILo	β=3.6074	399.57	403.57	406.00	0.1414	0.8349	0.2359	0.104
	θ=162.84							
IL	θ=584.84	399.57	401.57	402.79	0.1601	0.8452	0.2346	0.128

Table 7: MLEs and different statistics of the MAPTLo distribution and other models for the third dataset.

Model	Parameters	-2L	AIC	BIC	CM	AD	K-S	p-value
MAPTLo	α=36.83	284.26	290.26	297.25	0.0848	0.5387	0.0615	0.9358
	β=37.11							
	θ=1.29							
APTLo	α=6.528	284.62	290.62	297.61	0.0883	0.5749	0.0676	0.8771
	β=0.885							
	θ=1.651							
APTILo	α=4.8905	288.130	294.13	301.12	0.1260	0.8505	0.1128	0.2880
	β=0.0044							
	θ=80.992							
APTIL	α=22.106	297.303	301.303	305.964	0.183	1.142	0.1498	0.0658
	θ=0.4869							
Lo	β=0.1901	284.68	288.68	293.34	0.0869	0.5669	0.0733	0.8087
	θ=3.577							
ILo	β=0.4195	285.48	289.48	294.14	0.0935	0.6173	0.0741	0.7969
	θ=2.1439							
IL	θ=0.80158	316.844	318.844	321.175	0.2819	1.8001	0.2406	0.0003

Table 8: The CIs for α, β, and θ using the three real datasets.

Data/ Parameters	α	β	θ
First data	(5.188, 63.641)	(0.203, 0.558)	(3.833, 4.7167)
Second data	(0.00, 303.296)	(0.00, 0.0257)	(2.284, 2.918)
Third data	(13.726, 59.938)	(13.711, 60.506)	(1.263, 1.324)

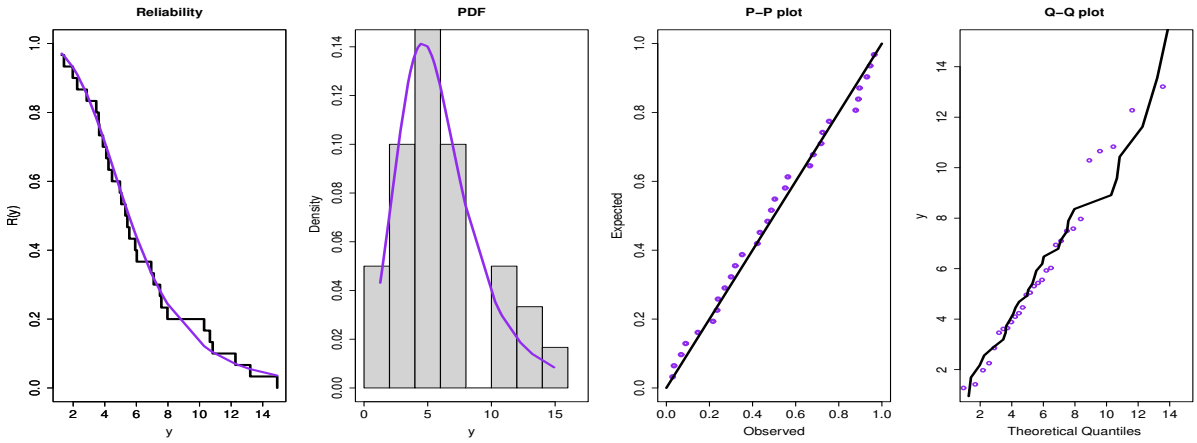


Figure 12: Plots of the fitted functions for the MAPTLo distribution of the first dataset.

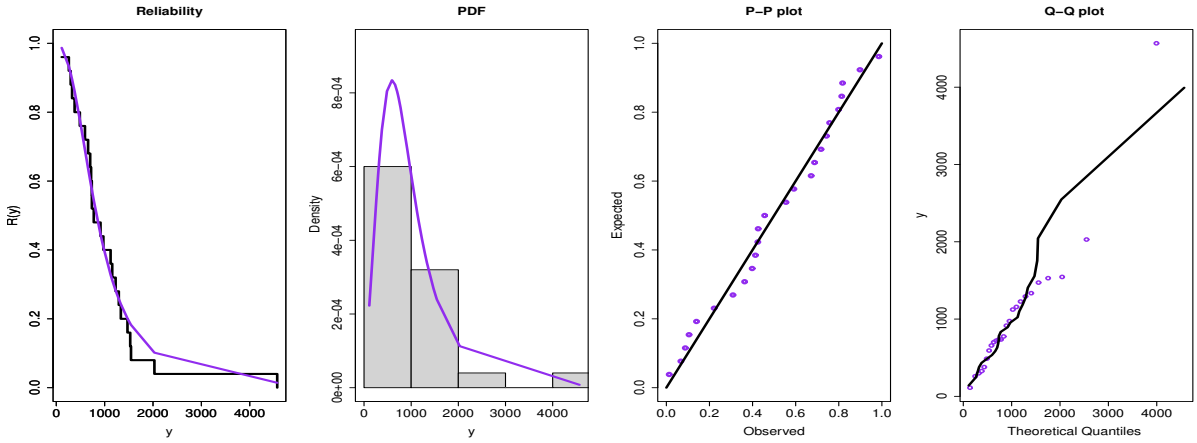


Figure 13: Plots of the fitted functions for the MAPTLo distribution of the second dataset.

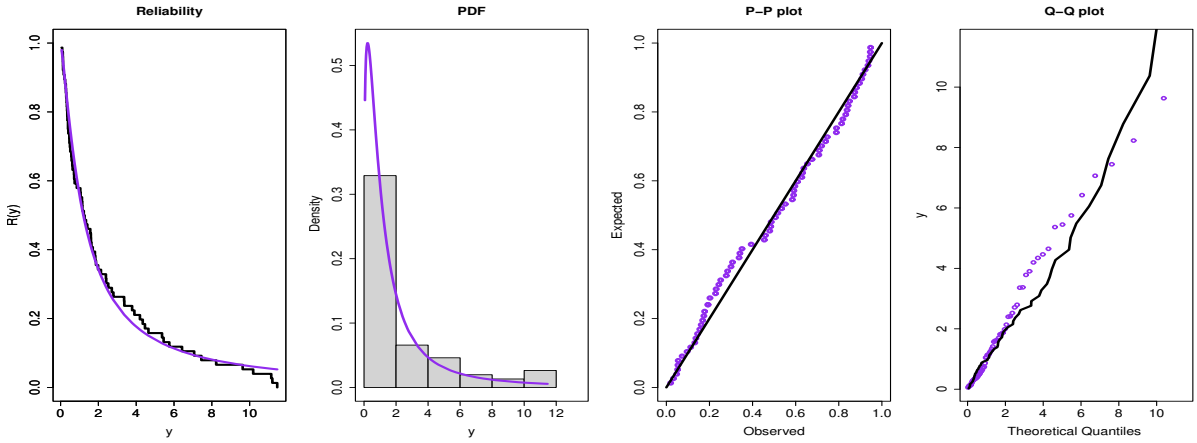


Figure 14: Plots of the fitted functions for the MAPTLo distribution of the third dataset.

7 Conclusion

The current research work has introduced a new extended distribution, named the modified alpha power transformed Lomax distribution through the alpha-power transformation of the Lomax distribution.

The statistical properties and reliability functions of the new distribution, including the quantile function, moments, entropies, order statistics, hazard rate function, mean residual life, and stress-strength reliability, have been provided. The maximum likelihood estimation method was also addressed to estimate the parameters of the new distribution. The simulation results support that the maximum likelihood estimation method provides competitive mean squared error and bias values for estimating the parameters. Three real-world datasets have been applied to demonstrate that the new distribution provides a better fit than many other competitive distributions, including the Lomax distribution. Therefore, it can be used for reliability inference and may provide directions for future research work.

Funding Statement

The author declared that no specific funding was received for this work.

Data Availability

The data that support the findings of this study are available within the paper.

Conflicts of Interest:

The author declares no conflicts of interest regarding this study.

Author Contributions

The author is solely responsible for all components of this work.

AI Usage Statement:

No AI-based tools were used in the generation, writing, revising, analysis, or interpretation of the research data and findings presented in this article.

Abbreviations

Abbreviation	Definition
AD	Anderson-Darling.
AIC	Akaike information criterion.
APT	Alpha power transformation.
BIC	Bayesian information criterion.
CDF	Cumulative distribution function.
CM	Cramér-von Mises.
CMs	Conditional moments.
HRF	Hazard rate function.
IMs	Incomplete moments.
Lo	Lomax.
MAPT	Modified alpha power transformation.
MIT	Mean inactivity time.
MLE	Maximum likelihood estimation.
MRL	Mean residual life.
MSE	Mean squared error.
PDF	Probability density function.
RF	Reliability function.
RHR	Reverse hazard rate.

References

[1] Lomax, K. S. (1954). Business failure: Another example of the analysis of the failure data. Journal of the American Statistical Association, 49(268), 847-852. doi:10.2307/2281544.

[2] Ghitany, M., Al-Awadhi, F., & Alkhalfan, L. (2007). Marshall–Olkin extended Lomax distribution and its application to censored data. Communications in Statistics—Theory and Methods, 36, 1855-1866. doi:10.1080/03610920601126571.

[3] Rajab, M., Aleem, M., Nawaz, T., & Daniyal, M. (2013). On five-parameter beta Lomax distribution. Journal of Statistics, 20(1), 102-118.

[4] Ashour, S. K., & Eltehiwy, M. A. (2013). Transmuted Lomax distribution. American Journal of Applied Mathematics and Statistics, 1(6), 121-127. doi:10.12691/ajams-1-6-3.

[5] El-Bassiouny, A. H., Abdo, N. F., & Shahen, H. S. (2015). Exponential Lomax distribution. International journal of computer applications, 121(13), 24-29. doi:10.5120/21602-4713.

[6] Tahir, M. H., Hussain, M. A., Cordeiro, G. M., Hamedani, G. G., Mansoor, M., & Zubair, M. (2016). The Gumbel Lomax distribution: properties and applications. Journal of Statistical Theory and Applications, 15(1), 61-79. doi:10.2991/jsta.2016.15.1.6.

[7] Zubair, M., Cordeiro, G. M., Tahir, M. H., Mahmood, M., & Mansoor, M. (2017). A study of Logistic-Lomax distribution and its applications. Journal of Probability and Statistical Science, 15(1), 29-46.

[8] Hassan, A. S., & Abd-Allah, M. (2018). Exponentiated Weibull-Lomax distribution: properties and estimation. Journal of Data Science, 16(2), 277-298. doi:10.6339/JDS.201804_16(2).0004.

[9] Elgohari H., & Yousof, H. (2020). A generalization of Lomax distribution with properties, copula and real data applications. Pakistan Journal of Statistics and Operation Research, 16(4), 697-711. doi:10.18187/pjsor.v16i4.3260.

[10] Ibrahim, S., Doguwa, S. I., Isah, A., & Jibril, H. M. (2021). Some properties and applications of topp Leone Kumaraswamy Lomax distribution. Journal of Statistical Modelling and Analytics, 3(2), 81-94. doi:10.22452/josma.vol3no2.5.

[11] Abu El Azm, W. S., Almetwally, E. M., Naji AL-Aziz, S., El-Bagoury, A. A. A. H., Alharbi, R., & Abo-Kasem, O. E. (2021). A new transmuted generalized Lomax distribution: properties and applications to COVID-19 data. Computational Intelligence and Neuroscience, 2021(1), 5918511. doi:10.1155/2021/5918511.

[12] Khan, S., Hamedani, G. G., Reyad, H. M., Jamal, F., Shafiq, S., & Othman, S. (2022). The minimum Lindley Lomax distribution: properties and applications. Mathematical and Computational Applications, 27(1), 1-16. doi:10.3390/mca27010016.

[13] Abiodun, A. A., & Ishaq, A. I. (2022). On Maxwell–Lomax distribution: properties and applications. Arab Journal of Basic and Applied Sciences, 29(1), 221-232. doi:10.1080/25765299.2022.2093033.

[14] Atchadé, M. N., A., Agbahide, A. A., Otodji, T., Bogninou, M. J., & Djibril. A. M. (2024). A new shifted Lomax-X family of distributions : properties and applications to actuarial and financial data. Computational Journal of Mathematical and Statistical Sciences, 4(1), 41–71. doi:10.21608/cjmss.2024.307114.1066.

[15] Abd Elgawad, M. A., Thampi, A., Swetha, P. S. S., & Nagarjuna, V. B. V. (2025). Weighted T-X power Lomax distribution: properties and applications in chemotherapy and economic. Journal of Radiation Research and Applied Sciences, 18, 101635. doi:10.1016/j.jrras.2025.101635.

[16] Afify, A. Z., Mahran, H. A., Alqawba, M., Aljohani, H. M., & Abdellatif, A. D. (2026). Properties and inference of the Pareto Lomax distribution with applications to real data. Scientific Reports, 16, 9082. doi:10.1038/s41598-026-43273-6.

[17] Mahdavi, A., & Kundu, D. (2017). A new method for generating distributions with an application to exponential distribution. Communications in Statistics–Theory and Methods, 46(13), 6543-6557. doi:10.1080/03610926.2015.1130839.

[18] Alotaibi, R., Okasha, H., Rezk, H., & Nassar, M. (2021). A new weighted version of alpha power transformation method: properties and applications to COVID-19 and software reliability data. Physica Scripta, 96(12), 125221. doi:10.1088/1402-4896/ac2658.

[19] Nassar, M., Alzaatreh, A., Mead, M., & Abo-Kasem, O. (2017). Alpha power Weibull distribution: properties and applications. Communications in Statistics–Theory and Methods, 46(20), 10236-10252. doi:10.1080/03610926.2016.1231816.

[20] Nassar, M., Kumar, D., Dey, S., Cordeiro, G. M., & Afify, A. Z. (2019). The Marshall–Olkin alpha power family of distributions with applications. Journal of Computational and Applied Mathematics, 315, 41-53. doi:10.1016/j.cam.2018.10.052.

[21] Eghwerido, J. T., Nzei, L. C., & Agu, F. I. (2021). The alpha power Gompertz distribution: characterization, properties, and applications. Sankhya A, 83(1), 449-475. doi:10.1007/s13171-020-00198-0.

[22] Dey, S., Nassar, M., & Kumar, D. (2019). Alpha power transformed inverse Lindley distribution: A distribution with an upside-down bathtub-shaped hazard function. Journal of Computational and Applied Mathematics, 348, 130-145. doi:10.1016/j.cam.2018.03.037.

[23] Basheer, A. M. (2019). Alpha power inverse Weibull distribution with reliability application. Journal of Taibah University for Science, 13(1), 423-432. doi:10.1080/16583655.2019.1588488.

[24] Basheer, A. M. (2022). Marshall-Olkin alpha power inverse exponential distribution: properties and applications. Annals of data science, 9(2), 301-313. doi:10.1007/s40745-019-00229-0.

[25] Almetwally, E. M., Sabry, M. A. H., Alharbi, R., Alnagar, D., Mubarak, S. A. M., & Hafez, E. H. (2021). Marshall–Olkin alpha power Weibull distribution: different methods of estimation based on type-I and type-II censoring. Complexity, 2021, 1-18. doi:10.1155/2021/5533799.

[26] ZeinEldin, R. A., Ahsan ul Haq, M., Hashmi, S., & Elsehety, M. (2020). Alpha power transformed inverse Lomax distribution with different methods of estimation and applications. Complexity, 2020(1), 1860813. doi:10.1155/2020/1860813.

[27] Maruthan, S. K., & Venkatachalam, N. (2022). Alpha power transformation of Lomax distribution: properties and applications. Thailand Statistician, 20(3), 669-685. `https://ph02.tci-thaijo.org/index.php/thaistat/article/view/246996`.

[28] Klakattawi, H. S., Aljuhani, W. H., & Baharith, L. A. (2022). Alpha power exponentiated new Weibull-Pareto distribution: its properties and applications. Pakistan Journal of Statistics and Operation Research, 18(3), 703-720. doi:10.18187/pjsor.v18i3.3937.

[29] Alsolmi, M. M., Almulhim, S. A., Amine, M. M., Aljohani, H. M., Alrumayh, A., & Belouadah, F. (2024). Statistical analysis and several estimation methods of new alpha power-transformed Pareto model with applications in insurance. Symmetry, 16(10), 1367. doi:10.3390/sym16101367.

[30] Bleed, S. O., Attwa, R. A., Ali R. F. M., & Radwan, T. (2024). On alpha power transformation generalized Pareto distribution and some properties. Journal of Applied Mathematics, 2024(1), 13. doi:10.1155/2024/6270350.

[31] Alotaibi, R., Okasha, H., Nassar, M., & Elshahhat, A. (2023). A novel modified alpha power transformed Weibull distribution and its engineering applications. Computer Modeling in Engineering & Sciences, 135, 2065-2089. doi:10.32604/cmes.2023.023408.

[32] Basheer, A. M., Al-Garash, S., & Modhesh, A. A. (2025). On the modified alpha power transformed Kumaraswamy distribution: properties and applications. Journal of Statistics Applications & Probability, 14(2), 225-240. doi:10.18576/jsap/140207.

[33] Basheer, A. M. (2025). New version of inverse Lindley distribution and its properties and applications. Albaydha University Journal, 7(1), 1061-1073. doi:10.56807/buj.v7i1.770.

[34] Rényi, A. (1961). On measures of entropy and information. In *Proceedings of the 4th Berkeley Symposium on Mathematical Statistics and Probability* (Vol. 1, pp. 547-561). University of California Press, Berkeley.

[35] Tsallis, C. (1988). Possible generalization of Boltzmann-Gibbs statistics. Journal of Statistical Physics, 52(1), 479-487. doi:10.1007/BF01016429.

[36] Pham, H. (2003). Accelerated life testing. In H. Pham (Ed.), *Handbook of Reliability Engineering* (Vol. 1). Springer, London. doi:10.1007/1-85233-841-5_22.

[37] Mubarak, A. E., & Al-Metwally, E. M. (2021). A new extension exponential distribution with applications of COVID-19 data. Journal of Financial and Commercial Research, 22(1), 444-460. doi:10.21608/jsst.2021.51484.1178.

[38] Akaike, H. (1974). A new look at the statistical model identification. IEEE Transactions on Automatic Control, 19(6), 716-723. doi:10.1109/TAC.1974.1100705.

[39] Schwarz, G. (1978). Estimating the dimension of a model. The Annals of Statistics, 6(2), 461-464. `https://www.jstor.org/stable/2958889`.

Disclaimer / Publisher's Note:

The statements and data in all publications are solely those of the author(s) and contributor(s) and do not necessarily reflect the views of the publisher. The publisher accepts no responsibility for any injury to people or property resulting from any ideas, methods, instructions or products referred to in the content.